Inorganic Chemistry
Article
Cite This: Inorg. Chem. XXXX, XXX, XXX−XXX
pubs.acs.org/IC

Light-Activated Electron Transfer and Turnover in Ru-Modified Aldehyde Deformylating Oxygenases

Rajneesh K. Bains, Jessica J. Miller, Hannah K. van der Roest, Sheng Qu, Brad Lute, and Jeffrey J. Warren*

Department of Chemistry, Simon Fraser University, 8888 University Drive, Burnaby, British Columbia V5A 1S6, Canada

Supporting Information

ABSTRACT: Conversion of biological molecules into fuels or other useful chemicals is an ongoing chemical challenge. One class of enzymes that has received attention for such applications is aldehyde deformylating oxygenase (ADO) enzymes. These enzymes convert aliphatic aldehydes to the alkanes and formate. In this work, we prepared and investigated ADO enzymes modified with Ru^{II}(tris-diimine) photosensitizers as a starting point for probing intramolecular electron transfer events. Three variants were prepared, with Ru^{II}-modification at the wild type (WT) residue C70, at the R62C site in one mutant ADO, and at both C62 and C70 in a second mutant ADO protein. The single-site modification of WT ADO at C70 using a cysteine-reactive label is an important observation and opens a way forward for new studies of electron flow, mechanism, and redox catalysis in ADO. These Ru-ADO constructs can perform the ADO catalytic cycle in the presence of light and a sacrificial reductant. In this work, the Ru photosensitizer serves as a tethered, artificial reductase that promotes turnover of aldehyde substrates with different carbon chain lengths. Peroxide side products were detected for shorter chain aldehydes, concomitant with less productive turnover. Analysis using semiclassical electron transfer theory supports proposals for hopping pathway for electron flow in WT ADO and in our new Ru-ADO proteins.

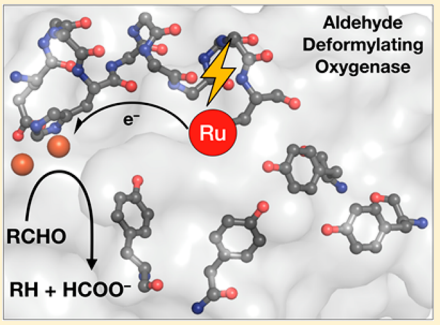

INTRODUCTION

Diiron cyanobacterial aldehyde deformylating oxygenase (ADO) enzymes have attracted attention for their unique chemistry and potential uses in the production of biofuels.[1] In natural systems, ADO enzymes convert fatty aldehydes to the corresponding C_{n-1} alkane and formate (eq 1).[2] In vivo, the aldehyde substrates derive from acyl-carrier proteins.[3,4] From the perspective of those aldehyde substrates, the overall reaction is redox neutral. However, turnover in ADO is coupled to the $4H^+/4e^-$ reduction of O_2 to two H_2O.[5] Remarkably, enzymatic cascades that include ADO can be integrated into synthetic metabolic pathways in other microbes to produce alkanes of various chain lengths, albeit in modest yields.[6,7] In vitro enzymatic assays display turnover rates near 1 min^{-1} using either chemical or protein-based reducing systems.[5,8,9]

$$RCH_2CHO + O_2 + 4H^+ + 4e^- \rightarrow RCH_3 + HCO_2H + H_2O \quad (1)$$

The reaction catalyzed by ADO (eq 1) requires four single electron transfer (ET) steps. The natural reductase for ADO is not yet known, but a recent report showed that a cyanobacterial 2Fe-2S ferredoxin (petF) is an effective reductant of the diferric active site with a rate constant of ~400 s^{-1}.[10] This ferredoxin is superior to other chemical reduction systems[5,8,9] and shows that enzymatic ET is faster than observed turnover frequencies. In this context, ET is not a rate-limiting step in ADO catalysis. In related mechanistic work, radicals were shown to form at Tyr (Y) and Cys (C) residues and mutations to those residues affect aldehyde yields.[10] Those Y and C radicals are on a pathway that extends from surface residues C70 to the iron(Fe_B)-ligating His63 (Figure 1).[10] Crystallographic data[11] and computational[12] analyses of the active site suggests that His attached to Fe_B is dynamically ligated and depends on the redox state of the

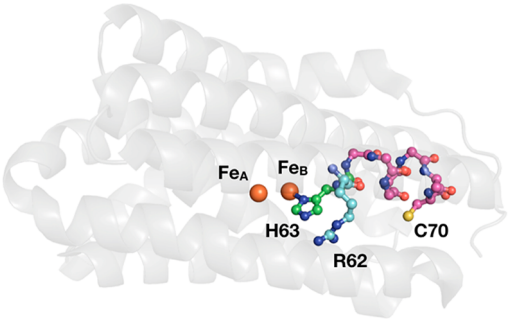

Figure 1. Structure of ADO from *S. elongatus* PCC7942 (PDB ID 4RC5). The diiron site is shown as orange spheres, H63 is in green, the site of mutation at R62 is in cyan, and the α-helix that connects C70 and the iron site is in magenta.

Received: March 17, 2018

DOI: 10.1021/acs.inorgchem.8b00673
Inorg. Chem. XXXX, XXX, XXX−XXX

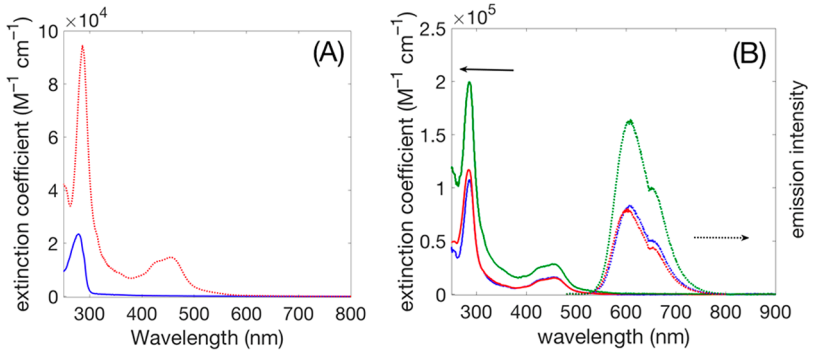

Figure 2. (A) Optical spectra of **Ru** (red dashed) and wild-type ADO (blue solid). (B) Optical (solid) and fluorescence (dashed) spectra of **Ru**-ADO proteins: **Ru**-C70 (blue), **Ru**-C62 (red), and **Ru**-C62/**Ru**-C70 (green). The arrows indicate axes corresponding to each set of spectra. Additional optical spectra are given in the Supporting Information.

active site. Ligands on Fe_A appear to be static. The His coordination behavior highlights the importance of Fe_B and is consistent with a mechanism that could involve ET (likely via hopping) from the ADO surface near C70 to the iron active site.[13,14] Further support for a hopping mechanism comes from the observation of Y and C radicals during turnover,[10] where these are likely derive from chemistry carried out in the Fe active site.[15] However, to learn more about intramolecular ET in ADO enzymes, new models are needed that allow for rapid initiation of redox reactions. To address this, we integrated Ru-tris(diimine) photosensitizers at two different sites on the surface of ADO. Herein we describe the preparation, characterization, and turnover characteristics of Ru-ADO proteins.

EXPERIMENTAL SECTION

Materials and Instrumentation. Solvents and buffer salts were from J. T. Baker unless otherwise noted. $RuCl_3$ was from Pressure Chemical. *cis*-Dichlororuthenium(2,2′-bipyridyl)$_2$ ($Cl_2Ru(bpy)_2$)[16] and (4-bromomethyl-4′-methyl-2,2′-bipyridyl)(2,2′-bipyridyl)$_2Ru^{II}(PF_6)2$ (denoted **Ru**)[17] were prepared according to the literature. Full details are given in the Supporting Information. Nickel nitrilotriacetic acid resin was from Thermo Fisher. All other chromatography media was from GE Healthcare. Polymerase chain reaction (PCR) primers were purchased from Eurofins Operon. Restriction enzymes and Q5 DNA polymerase were from New England Biolabs. Plasmid DNA was isolated using a Qiagen Spin Miniprep kit.

UV−Visible spectra were obtained using either a Photon Control SPM-002-EH CCD with an SPLC 1DH deuterium/tungsten light source or a Cary 100-Bio UV−visible spectrometer. A Bruker microFLEX MALDI-TOF instrument with a 48-well ground steel target was used for all mass spectrometry (MS) experiments. The dried droplet method was used with sinapinic acid as the matrix. Theoretical molecular weights are obtained from the protein sequence using ExPASy: Compete Pi/MW tool.[18] Circular dichroism spectra were collected using a Chirascan qCD spectrometer and converted using the following formula $[\theta] = \theta M_r/(nCl)$, where M_r, n, C, and l represent molecular weight (Da), number of residues, concentration (in mg/mL), and the cuvette path length, respectively. Fluorescence spectra were collected on Jobin-Yvon FluoroLog3 fluorometer. All samples were deoxygenated using repeated pump-purge cycles with argon backfill. Samples were excited at 455 nm. NMR experiments were performed using a Bruker AVANCE III 500 MHz running IconNMR under TopSpin 2.1. A Simpson water suppression pulse program was used for all aqueous NMR experiments. Gas chromatography-mass spectrometry (GC-MS) experiments were performed using an Agilent 6890 series gas chromatograph with 5973 Network Mass Selective Detector equipped with a capillary DB-5 column (0.25 mm × 30m × 0.25 μm).

The codon-optimized gene for *Synechococcus elongatus* ADO was a gift from D. Baker (University of Washington). The ADO mutants (R62C and R62C/C70S/C116S) were prepared using the Agilent Quikchange protocol. Introduction of the desired mutations was confirmed from DNA sequencing performed by Eurofins Operon. Protein expression and purification was performed using standard procedures (see Supporting Information).

For Ru-labeling, 1,4-dithiothreitol (DTT) was added to ADO solutions to a final concentration of 20 mM and incubated at room temperature for at least 45 min. DTT was removed using a PD-10 desalting column. **Ru** was dissolved in dimethyl sulfoxide (DMSO) and added (1.2 equiv for single labeling and 2.4 equiv for double labeling) to 60 μM protein solutions, and the resulting mixtures were stirred in the dark at 4 °C overnight. Final DMSO concentrations were 1%. No precipitation was observed during incubation. Optimization of the protocol showed that 60 μM protein with a 20% excess of **Ru**-label and a 12 h labeling time (12 h vs 4 or 8 h) gave the highest and most reproducible yields (70+%). Labeling at room temperature was more rapid but also resulted in some protein precipitation. Crude **Ru**-modified protein solutions were exchanged into 5 mM 4-(2-hydroxyethyl)-1-piperazineethanesulfonic acid (HEPES; pH 7.6) using a PD-10 column and loaded onto an FPLC DEAE Hi-Prep column eluted with an increasing NaCl gradient. Fractions containing **Ru**-labeled protein were pooled and exchanged into 50 mM sodium phosphate, 100 mM NaCl, pH 7.5 using a PD-10 column. Protein samples were stored in the dark at 4 °C. Typical isolated yields of Ru-modified proteins ranged from 30 to 50%. Labeling was confirmed using UV−visible spectroscopy and trypsin digestions (see Supporting Information).

Photochemical reaction mixtures contained 10 μM Ru-ADO + 10 mM sodium diethyldithiocarbamate (DTC) in 50 mM sodium phosphate and 100 mM NaCl (pH 7.5) buffer. Ru-ADO was mixed with 2 mol equiv of ferrous ammonium sulfate prior to reactions. For all reactions, a single reaction mixture was split into two aliquots, where one was shielded from light. The remaining mixture was exposed to visible light from a Kodak extra bright lamp projector source. Mixtures were stirred continuously in a temperature-controlled water bath. Prior to NMR analysis, reaction solutions were centrifuged briefly to remove insoluble oxidized DTC, and 10% (v/v) D_2O was added. The solution was then transferred to NMR tubes (5 mm diameter), and NMR spectra were collected. Ethyl acetate-extracted aqueous reaction mixtures were analyzed using GC-MS. Full descriptions of protocols are given in the Supporting Information.

RESULTS

Analysis of the X-ray structure of ADO from *S. elongatus* strain PCC7942[19] reveals the presence of three C (residues 70, 106, 116). Of those, C70 and C116 are the most exposed to solvent. Cysteine-reactive (4-bromomethyl-4′-methyl-2,2′-bipyridyl)-(2,2′-bipyridyl)$_2Ru^{II}(PF^6)_2$ (denoted as **Ru**) was used to

DOI: 10.1021/acs.inorgchem.8b00673
Inorg. Chem. XXXX, XXX, XXX−XXX

modify the proteins described in this work; such Ru-complexes have been used in several studies of ET in metalloproteins.[20−22] Surprisingly, treatment of WT ADO with **Ru**[23] results in a single cysteine modification. Trypsin digestion and analysis of the fragments using mass spectrometry reveals that C70 is the modified site (see Supporting Information). Site-directed mutagenesis was also used to produce two other mutant ADO proteins: R62C and R62C/C70S/C116S. Residue 62 was chosen for modification because it is surface-exposed and connected directly to the Fe active site via His63. As shown in Ru-modified cytochromes P450, the site of labeling is an important factor in photochemical enzyme activity.[24] Treatment of R62C ADO with **Ru** yields a protein modified at both C62 and C70, as confirmed by trypsin digestion experiments, while the R62C/C70S/C116S variant is only labeled once (**Ru**-C62). Circular dichroism spectra of unlabeled mutants and **Ru**-modified analogues are nearly identical, suggesting that that **Ru**-labeling does not dramatically alter ADO's helical secondary structures. Analogous mutations to WT Cys residues are known in *Nostoc punctiforme* ADO, and these mutations thermally destabilize the protein by ca. 6 °C, but the secondary structures are not strongly affected.[25] Finally, **Ru** modification of WT ADO lowers the melting temperature by ∼3 °C (see Supporting Information).

The optical and fluorescence spectra (Figure 2) of **Ru**-ADO proteins show characteristic metal-to-ligand charge transfer (MLCT) absorption bands, and the maximum emission intensity is at 600 nm (with 455 nm excitation). There is a slight red shift in absorbance between the **Ru**-modified proteins (λ_{max} = 458 nm) and the label (λ_{max} = 455 nm). The intensity of the MLCT band is proportional to the number of **Ru** labels. The extinction coefficients at 455 nm are ε (**Ru**-C70) = 14 500 M^{-1} cm^{-1}, ε (**Ru**-C62) = 14 500 M^{-1} cm^{-1}, and ε (**Ru**-C62/**Ru**-C70) = 29 000 M^{-1} cm^{-1}, based on spectra of related ruthenium polypyridyl complexes.[26] Additional UV−visible spectra are given in the Supporting Information. The normalized fluorescence maxima show the same trend. The observed luminescence decay time constants (τ) in oxygenated buffer for *Ru are 102 ns (**Ru**-C70), 78 ns (**Ru**-C62), and 51 ns (**Ru**-C62/**Ru**-C70) (see Supporting Information). For comparison, the lifetime for *$Ru(bpy)_3^{2+}$ is 140 ns under the same conditions ($Ru(bpy)_3^{2+}$ = tris(2,2′-bipyridyl)ruthenium dication).

Electronically excited *Ru^{II} complexes can be quenched by sacrificial electron donors to yield the corresponding reduced Ru complex.[27] Reduced **Ru** is a strong reductant, with $E^{o\prime}$ near −1.2 V versus the normal hydrogen electrode (NHE).[28] Here, DTC was used as the sacrificial quencher. The low water solubility and limited reactivity of the DTC oxidation product (disufiram) make it useful in investigation of protein photocatalysis.[22,23] Addition of 10 mM DTC to 10 μM solutions of **Ru**-ADO in 50 mM sodium phosphate and 100 mM sodium chloride, pH 7, quenches the steady-state luminescence of all proteins by ca. 60% (spectra are shown in the Supporting Information).

Next, the ability of **Ru**-ADO to turn over using light and sacrificial reductants was investigated. Aqueous solutions containing 10 μM **Ru**-ADO, 10 mM DTC, and saturating undecanal (∼160 μM) in 50 mM sodium phosphate, 100 mM sodium chloride, pH 7.5, were irradiated for up to 60 min at room temperature using a halogen light source with a UV cutoff filter (λ > 380 nm). During irradiation, a white precipitate formed, consistent with formation of the disulfiram product expected from DTC quenching of *Ru^{II}. Analysis using ^{1}H NMR (see Supporting Information) also shows formation of a downfield singlet at 8.35 ppm (Figure 3). This

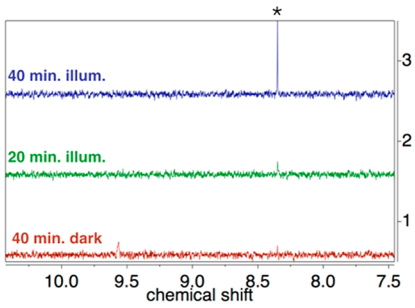

Figure 3. ^{1}H NMR spectra of 10 μM **Ru**-C70 ADO samples under photocatalytic conditions using undecanal as substrate. Spectrum 1 (bottom) is a dark control, and spectra 2 (middle) and 3 (top) were collected after 20 and 40 min of illumination, respectively. The * indicates the chemical shift of $HCOO^-$.

peak was assigned to formate based on spiking with authentic sample and comparison to external standards. The control (dark) samples routinely showed formation of trace formate over the course of 40 min, which we attribute to the weak reducing power of DTC, which is present in large excess.

Integrated peak areas suggest formation of 40 ± 10 μM (5 ± 2 mg/L) over the course of 60 min of irradiation. This places an upper limit on formate production of **Ru**-ADO near 0.7 μM min^{-1}, consistent with other chemical reducing systems.[29] Identical samples kept in the dark show no disulfiram precipitate or almost no production of formate (see above). Production of formate also was detected with aldehydes of varying chain lengths ranging from C_6 to C_{11} (with the exception of C_9, which was not tested). The substrate specificity and turnover properties of ADO with these other chain lengths has been investigated elsewhere in detail.[30]

Control reactions where any one of the reaction components (**Ru**-ADO, DTC, or aldehyde) were omitted showed no production of formate. Octanal was used as a test substrate due to its higher water solubility. Following literature examples of photoreduction of proteins using noncovalently bound $Ru(bpy)_3Cl_2$,[31] addition of $Ru(bpy)_3Cl_2$ in a 1:1 molar ratio with unmodified WT ADO, and all other reaction components, shows production of trace formate (<1 μM). In this control, consumption of DTC was observed. These experiments demonstrate that covalent attachment of **Ru** to ADO is important for function.

When using aldehydes shorter than C_{11}, other products were detected using ^{1}H NMR and GC-MS at reaction times greater than 20 min. For example, GC-MS analyses showed trace production of alcohols, as is known for ADO.[32] At those longer reaction times, and with shorter aldehydes (C_6−C_8), a resonance at 9.1 ppm also was observed in ^{1}H NMR spectra. This chemical shift suggests production of hydroperoxide-containing compounds. This hypothesis is consistent with detection of alkyl peroxyl radicals during ADO turnover.[10] To confirm peroxide production, postillumination reaction mixtures were extracted with PPh_3 in $CDCl_3$ and analyzed using ^{31}P NMR. A ^{31}P NMR resonance at 29 ppm was observed (see Supporting Information), which was confirmed as $OPPh_3$ by spiking with authentic sample. The modest turnover on **Ru**-ADO can be partially attributed to production

DOI: 10.1021/acs.inorgchem.8b00673
Inorg. Chem. XXXX, XXX, XXX−XXX

of these side products. Any production of hydrogen peroxide also could inhibit turnover.[8]

GC-MS was used to identify the decane produced from decarbonylation of undecanal by **Ru**-ADO. The decane product was extracted using ethyl acetate. The yields assayed using GC-MS were: 2.1 ± 0.1 (**Ru**-C62/**Ru**-C70), 2.0 ± 0.1 (**Ru**-C70), and 0.6 ± 0.1 (**Ru**-C62) mg/L, respectively. The apparent yields of alkanes are somewhat lower than for formate, which we attribute to inefficiencies in the extraction protocol. The NMR experiments do not require extraction and are a better measure of true yields. Notably, the production of formate and decane for **Ru**-C62 ADO (with a C70S mutation) is significantly (ca. 70%) lower than the other two **Ru**-ADO models with **Ru** at C70. In recent work, the C71A variant of *N. punctiforme* ADO (analogous to residue C70 in this work) showed a 27% reduction in activity with respect to the WT protein, demonstrating the importance of that cysteine residue for ADO function.[10] Overall, the two **Ru**-ADO proteins with **Ru** at C70 show greater activity than the variant labeled only at C62.

DISCUSSION

WT ADO can be readily modified at the surface-exposed residue C70 using a thiol-reactive ruthenium(II) complex. This was the only detected labeled product, although there is another partially exposed cysteine (C116) in the WT protein. It is surprising that covalent modification at ADO-C70 with a redox-active molecule does not affect the ability of the enzyme to turn over under photocatalytic conditions. In contrast, elimination of this residue and attachment of **Ru** elsewhere (in **Ru**-C62 ADO) impairs the ability of ADO to function. Generation of a strong **Ru** reductant near the active site (as in **Ru**-C62) is insufficient to give an active enzyme. We note that ET from both the **Ru**-C62 site and the **Ru**-C70 site to the Fe active site likely involves the peptide backbone that connects the **Ru**-label to the Fe-ligated His63. In this context, it is notable that single-**Ru** modification at C62 and C70 result in markedly different abilities of the resulting ADO to produce formate. This underscores the importance of the ET pathway involving C70 and suggests that future investigations of function ET in these **Ru**-modified proteins must account for this feature.

The **Ru**-modified ADO described here is active, but the activity is low with respect to other assays that employ weaker reductants than **Ru** (E° = −1.2 V). Side reactions of **Ru** are problematic and account, in part, for this observation. More DTC is consumed than can be accounted for by the $4e^-$ stoichiometry required by ADO, which could be due to adventitious reactions of electronically excited **Ru**[33] or reduced **Ru** with O_2. In addition, atmospheric concentrations of O_2 have been shown to inhibit catalysis by ADO,[7,8,34] consistent with our observed production of peroxides in **Ru**-ADO under photocatalytic conditions (see above).

The above observations motivated us to analyze ET pathways and energetics in ADO and **Ru**-ADO proteins. Inspection of the X-ray structures of ADO enzymes shows a series of tyrosine residues that extend from the iron site to the surface of the protein, near C70 (e.g., Figure 4). This "chain" of Y residues is structurally conserved across ADO enzymes from different organisms[35] and is widely conserved in aligned protein sequences from ADO enzymes from different species (see Supporting Information). In addition, the chain of redox-active Tyr residues resembles those that are proposed to play

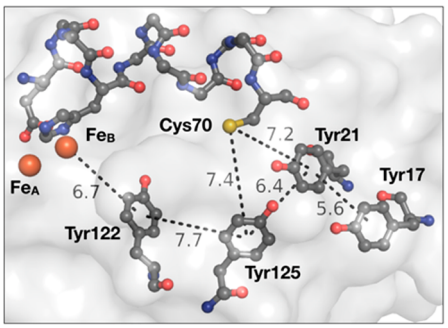

Figure 4. Illustration of the Y chain that extends from the *S. elongatus* ADO Fe site to the protein surface (C70 or Y17). The peptide connecting **Ru** to the Fe active site in **Ru**-ADO is shown at the top. Distances are to/from aromatic ring centers. PDB ID 4RC5.

protective roles in other metalloenzymes.[36] This could be an interesting example of a case where such a chain plays a direct functional role in enzyme catalysis. In ADO, this series of residues may play a role in turnover that is reminiscent of electron transport in some ribonucleotide reductases (RNRs).[37] Some of these Y residues were identified as sources of radicals for ADO under turnover conditions, and mutations to those Y reduced, but did not destroy, ADO catalytic activity.[10] Residue C70 is situated near the protein surfaces and is about equidistant from Y125 and Y21. In the following paragraphs, we analyze potential ET pathways in the context of natural and **Ru**-ADO.

Recent elucidation of the energetics of ET via tyrosine residues in RNR[38,39] inspired us to analyze multistep ET in ADO using semiclassical ET theory (eq 2), which is a typical starting point for understanding ET reactions in proteins.[14] Much work is left to be done in ADO, but the following analysis is a starting point. The following analysis uses typical ET parameters for proteins: λ = 0.8 eV and $H_{AB} = H_{AB}{}^0\exp(-\beta r)$, where $H_{AB}{}^0$ = 186 cm^{-1}, β = 1.1 $Å^{-1}$, and r is the distance between cofactors.[40] H_{AB} is the electronic coupling strength of the reactants and products at the transition state, and β is the distance decay constant.[40] Additional details about these calculations are given in the Supporting Information. Given the complexity of the ET chain in ADO, some limiting cases are presented here to demonstrate the importance of electron flow through Y and/or C.

$$k_{ET} = \sqrt{\frac{4\pi^3}{h^2\lambda k_B T}}\, H_{AB}{}^2 \exp\left(\frac{-(\Delta G^\circ + \lambda)^2}{4\lambda k_B T}\right) \quad (2)$$

An upper limit for the potentials of activated intermediates can be approximated as 1.4 V based on the potentials for alkyl radicals[41] or for related Fe model compounds.[42] The proton-coupled potential for C−S·/C−SH at pH 7 is 0.82 V, and that for Y−O·/Y−OH is 0.83 V. Likewise, E°(C−S·/C−S^-) = 0.73 V, and E°(Y−O·/Y−O^-) = 0.65 V.[41] Thus, the driving force (−ΔG°) for ET from a surface residue (C or Y) of WT ADO (unmodified with **Ru**) to the active site is estimated as less than or equal to 0.75 V.[43] Given the nature of the iron or organic intermediates, it is unlikely that the *net* reaction is thermodynamically uphill, but any individual step could be. Given a limiting value of $-\Delta G^\circ$ = −200 meV,[14,38] ET could proceed at 2 × 10^5 s^{-1} with tunneling distances under 8 Å (using eq 2).

DOI: 10.1021/acs.inorgchem.8b00673
Inorg. Chem. XXXX, XXX, XXX−XXX

Direct reduction of intermediate alkyl radicals, either by **Ru** ($E^\circ = -1.2$ V) or ferredoxin,[10] is unlikely, as there is evidence that the H· atom required to form the alkane product comes from the ADO active site.[10,29] **Ru** is a strong reductant, so the driving force for ET is deeply in the Marcus inverted region, with $k_{calc} \ll 1\ s^{-1}$ ($r \approx 20$ Å, as an estimate of the **Ru**–**Fe** distance). In contrast, milder reductants, such as petF ferredoxin ($E^{\circ\prime} = -0.412$ V[44]) or DTC ($E^{\circ\prime} \approx -0.3$ V[45]), can be orders of magnitude faster simply due to their weaker reducing power with respect to **Ru**. In contrast, **Ru** is predicted to be a good reductant for the ferric ADO resting state. The reduction potential for the $Fe^{III}Fe^{III}$ resting state is not yet known, but our estimate is between −0.1 and 0.3 V based on potentials for related diiron enzymes.[46−48] Reduction of the $Fe^{III}Fe^{III}$ site can have a single-step **Ru** → Fe ET rate that is at least as fast as reduction by ferredoxin ($400\ s^{-1}$). A proposed cycle for **Ru**-ADO accounting for this ET analysis is set out in Figure 5.

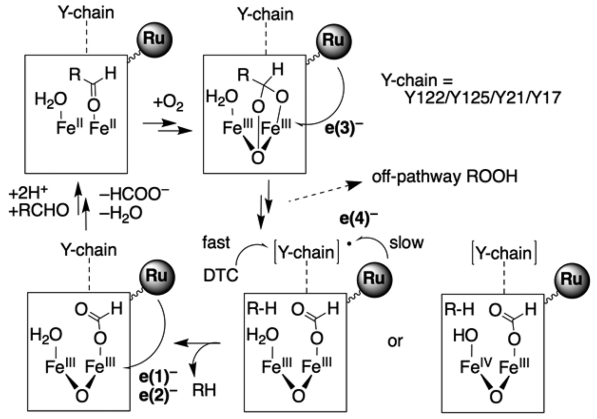

Figure 5. Proposed catalytic cycle for electron delivery in **Ru**-ADO proteins. The sequential addition of electrons are denoted as $e(n)^-$ (n = 1−4).

There are still many questions about ET in ADO enzymes. The following suggestions can be made regarding functional ET in **Ru**- and WT-ADO based on the above analysis. **Ru** can act as a reductant for oxidized ADO, but it is probably not a suitable reductant for other intermediates. The milder reduction potential of ferredoxins (such as petF) are more appropriate to support catalysis. In that context, DTC is a probable reductant of **Ru**-ADO intermediates in the present work. Finally, the comparatively low activity of **Ru**-C62 ADO can be attributed to the position of **Ru** with respect to the natural Y/C ET chain. During turnover, holes are funneled away from **Ru**-C62. ET to reduce any intermediates is in the inverted region and is calculated to be very slow from position 62 (in comparison to **Ru**-C70). Thus, to study functional ET in ADO, it is not sufficient to simply place a photosensitizer/reductant anywhere near the active site.

In sum, three different **Ru**-modified ADO proteins were characterized and evaluated for their ability to decarbonylate aliphatic aldehyde substrates under photocatalytic conditions. The order of increasing catalytic reactivity was: **Ru**-C70 ≈ **Ru**-C62/**Ru**-C70 > **Ru**-C62. Importantly, the unique reactivity of wild-type ADO C70 opens the door to new applications or investigations of electron flow during catalysis, for example, using time-resolved spectroscopies or electrochemistry. We are presently investigating the ability of oxidized **Ru** (Ru(III)) to oxidize ADO active sites or nearby redox-active amino acids. Our analysis of reductive ET suggests that photochemical ET to the diferric active site, generating the O_2-reactive diferrous enzyme, can occur readily with **Ru** as a reductant. Other intramolecular ET reactions are a possible pathway for ET from the surface of ADO to activated intermediates in the native ADO enzymes. Side reactions involving O_2 were identified as challenges in developing an ADO system with better photochemical activity.

■ ASSOCIATED CONTENT

Supporting Information

The Supporting Information is available free of charge on the ACS Publications website at DOI: 10.1021/acs.inorgchem.8b00673.

Detailed ADO expression and purification procedures, mass spectrometry and circular dichroism data, UV−visible and luminescence spectra, additional electron transfer analyses (PDF)

■ AUTHOR INFORMATION

Corresponding Author

*E-mail: j.warren@sfu.ca

ORCID

Jeffrey J. Warren: 0000-0002-1747-3029

Notes

The authors declare no competing financial interest.

■ ACKNOWLEDGMENTS

Simon Fraser Univ., the National Sciences and Engineering Research Council of Canada (NSERC, RGPIN05559 to J.J.W.), the Canada Summer Jobs program (Project No. 014504120 to J.J.W.), and the Canadian Institute for Advanced Research Azrieli Global Scholars and Bio-Inspired Solar Energy programs (to J.J.W.) supported this work. J.J.M. acknowledges support from NSERC and SFU for postgraduate fellowships. H.K.v.d.R. acknowledges support from the NSERC USRA program. N. Merbouh, S. Grunnert, and P. Mulyk assisted with GC-MS experiments. The plasmid encoding ADO was a gift from D. Baker.

■ REFERENCES

(1) Schirmer, A.; Rude, M. A.; Li, X.; Popova, E.; del Cardayre, S. B. Microbial Biosynthesis of Alkanes. *Science* **2010**, *329*, 559−562.

(2) Warui, D. M.; Li, N.; Nørgaard, H.; Krebs, C.; Bollinger, J. M.; Booker, S. J. Detection of Formate, Rather than Carbon Monoxide, As the Stoichiometric Coproduct in Conversion of Fatty Aldehydes to Alkanes by a Cyanobacterial Aldehyde Decarbonylase. *J. Am. Chem. Soc.* **2011**, *133*, 3316−3319.

(3) Lin, F.; Das, D.; Lin, X. N.; Marsh, E. N. G. Aldehyde-forming fatty acyl-CoA reductase from cyanobacteria: expression, purification and characterization of the recombinant enzyme. *FEBS J.* **2013**, *280*, 4773−4781.

(4) Warui, D. M.; Pandelia, M.-E.; Rajakovich, L. J.; Krebs, C.; Bollinger, J. M.; Booker, S. J. Efficient Delivery of Long-Chain Fatty Aldehydes from the Nostoc punctiforme Acyl-Acyl Carrier Protein Reductase to Its Cognate Aldehyde-Deformylating Oxygenase. *Biochemistry* **2015**, *54*, 1006−1015.

(5) Li, N.; Chang, W.-c.; Warui, D. M.; Booker, S. J.; Krebs, C.; Bollinger, J. M. Evidence for Only Oxygenative Cleavage of Aldehydes to Alk(a/e)nes and Formate by Cyanobacterial Aldehyde Decarbonylases. *Biochemistry* **2012**, *51*, 7908−7916.

DOI: 10.1021/acs.inorgchem.8b00673
Inorg. Chem. XXXX, XXX, XXX−XXX

(6) Howard, T. P.; Middelhaufe, S.; Moore, K.; Edner, C.; Kolak, D. M.; Taylor, G. N.; Parker, D. A.; Lee, R.; Smirnoff, N.; Aves, S. J.; Love, J. Synthesis of customized petroleum-replica fuel molecules by targeted modification of free fatty acid pools in Escherichia coli. *Proc. Natl. Acad. Sci. U. S. A.* **2013**, *110*, 7636−7641.
(7) Kallio, P.; Pásztor, A.; Thiel, K.; Akhtar, M. K.; Jones, P. R. An engineered pathway for the biosynthesis of renewable propane. *Nat. Commun.* **2014**, *5*, 4731.
(8) Andre, C.; Kim, S. W.; Yu, X.-H.; Shanklin, J. Fusing catalase to an alkane-producing enzyme maintains enzymatic activity by converting the inhibitory byproduct H_2O_2 to the cosubstrate O_2. *Proc. Natl. Acad. Sci. U. S. A.* **2013**, *110*, 3191−3196.
(9) Das, D.; Eser, B. E.; Han, J.; Sciore, A.; Marsh, E. N. G. Oxygen-Independent Decarbonylation of Aldehydes by Cyanobacterial Aldehyde Decarbonylase: A New Reaction of Diiron Enzymes. *Angew. Chem., Int. Ed.* **2011**, *50*, 7148−7152.
(10) Rajakovich, L. J.; Nørgaard, H.; Warui, D. M.; Chang, W.-c.; Li, N.; Booker, S. J.; Krebs, C.; Bollinger, J. M.; Pandelia, M.-E. Rapid Reduction of the Diferric-Peroxyhemiacetal Intermediate in Aldehyde-Deformylating Oxygenase by a Cyanobacterial Ferredoxin: Evidence for a Free-Radical Mechanism. *J. Am. Chem. Soc.* **2015**, *137*, 11695−11709.
(11) Buer, B. C.; Paul, B.; Das, D.; Stuckey, J. A.; Marsh, E. N. G. Insights into Substrate and Metal Binding from the Crystal Structure of Cyanobacterial Aldehyde Deformylating Oxygenase with Substrate Bound. *ACS Chem. Biol.* **2014**, *9*, 2584−2593.
(12) Wang, C.; Zhao, C.; Hu, L.; Chen, H. Calculated Mechanism of Cyanobacterial Aldehyde-Deformylating Oxygenase: Asymmetric Aldehyde Activation by a Symmetric Diiron Cofactor. *J. Phys. Chem. Lett.* **2016**, *7*, 4427−4432.
(13) Giese, B.; Wang, M.; Gao, J.; Stoltz, M.; Muller, P.; Graber, M. Electron relay race in peptides. *J. Org. Chem.* **2009**, *74*, 3621−3625.
(14) Warren, J. J.; Ener, M. E.; Vlcek, A., Jr.; Winkler, J. R.; Gray, H. B. Electron hopping through proteins. *Coord. Chem. Rev.* **2012**, *256*, 2478−2487.
(15) Paul, B.; Das, D.; Ellington, B.; Marsh, E. N. G. Probing the Mechanism of Cyanobacterial Aldehyde Decarbonylase Using a Cyclopropyl Aldehyde. *J. Am. Chem. Soc.* **2013**, *135*, 5234−5237.
(16) Sullivan, B. P.; Salmon, D. J.; Meyer, T. J. Mixed phosphine 2,2′-bipyridine complexes of ruthenium. *Inorg. Chem.* **1978**, *17*, 3334−3341.
(17) Berg, K.; Tran, A.; Raymond, M.; Abrahamsson, M.; Wolny, J.; Redon, S.; Andersson, M.; Sun, L.; Styring, S.; Hammarström, L.; Toftlund, H.; Åkermark, B. Covalently Linked Ruthenium(II)-Manganese(II) Complexes: Distance Dependence of Quenching and Electron Transfer. *Eur. J. Inorg. Chem.* **2001**, *2001*, 1019−1029.
(18) http://web.expasy.org/compute_pi/ (Accessed April 4, 2016).
(19) Jia, C.; Li, M.; Li, J.; Zhang, J.; Zhang, H.; Cao, P.; Pan, X.; Lu, X.; Chang, W. Structural insights into the catalytic mechanism of aldehyde-deformylating oxygenases. *Protein Cell* **2015**, *6*, 55−67.
(20) Berglund, J.; Pascher, T.; Winkler, J. R.; Gray, H. B. Photoinduced Oxidation of Horseradish Peroxidase. *J. Am. Chem. Soc.* **1997**, *119*, 2464−2469.
(21) Bjerrum, M. J.; Casimiro, D. R.; Chang, I. J.; Di Bilio, A. J.; Gray, H. B.; Hill, M. G.; Langen, R.; Mines, G. A.; Skov, L. K.; Winkler, J. R.; Wuttke, D. S. Electron transfer in ruthenium-modified proteins. *J. Bioenerg. Biomembr.* **1995**, *27*, 295−302.
(22) Tran, N.-H.; Nguyen, D.; Dwaraknath, S.; Mahadevan, S.; Chavez, G.; Nguyen, A.; Dao, T.; Mullen, S.; Nguyen, T.-A.; Cheruzel, L. E. An Efficient Light-Driven P450 BM3 Biocatalyst. *J. Am. Chem. Soc.* **2013**, *135*, 14484−14487.
(23) Tran, N.-H.; Huynh, N.; Bui, T.; Nguyen, Y.; Huynh, P.; Cooper, M. E.; Cheruzel, L. E. Light-initiated hydroxylation of lauric acid using hybrid P450 BM3 enzymes. *Chem. Commun.* **2011**, *47*, 11936−11938.
(24) Tran, N.-H.; Huynh, N.; Chavez, G.; Nguyen, A.; Dwaraknath, S.; Nguyen, T.-A.; Nguyen, M.; Cheruzel, L. A series of hybrid P450 BM3 enzymes with different catalytic activity in the light-initiated hydroxylation of lauric acid. *J. Inorg. Biochem.* **2012**, *115*, 50−56.
(25) Hayashi, Y.; Yasugi, F.; Arai, M. Role of Cysteine Residues in the Structure, Stability, and Alkane Producing Activity of Cyanobacterial Aldehyde Deformylating Oxygenase. *PLoS One* **2015**, *10*, e0122217.
(26) McClanahan, S. F.; Dallinger, R. F.; Holler, F. J.; Kincaid, J. R. Mixed-ligand poly(pyridine) complexes of ruthenium(II). Resonance Raman spectroscopic evidence for selective population of ligand-localized 3MLCT excited states. *J. Am. Chem. Soc.* **1985**, *107*, 4853−4860.
(27) Deronzier, A.; Meyer, T. J. Photoinduced reduction of tris(2,2′-bipyridine)ruthenium(2+) by some dithio anions. *Inorg. Chem.* **1980**, *19*, 2912−2917.
(28) Balzani, V.; Bolletta, F.; Gandolfi, M. T.; Maestri, M. Bimolecular electron transfer reactions of the excited states of transition metal complexes. *Top. Curr. Chem.* **1978**, *75*, 1−64.
(29) Waugh, M. W.; Marsh, E. N. G. Solvent Isotope Effects on Alkane Formation by Cyanobacterial Aldehyde Deformylating Oxygenase and Their Mechanistic Implications. *Biochemistry* **2014**, *53*, 5537−5543.
(30) Khara, B.; Menon, N.; Levy, C.; Mansell, D.; Das, D.; Marsh, E. N. G.; Leys, D.; Scrutton, N. S. Production of Propane and Other Short-Chain Alkanes by Structure-Based Engineering of Ligand Specificity in Aldehyde-Deformylating Oxygenase. *ChemBioChem* **2013**, *14*, 1204−1208.
(31) Nilsson, T. Photoinduced electron transfer from tris(2,2′-bipyridyl)ruthenium to cytochrome c oxidase. *Proc. Natl. Acad. Sci. U. S. A.* **1992**, *89*, 6497−6501.
(32) Aukema, K. G.; Makris, T. M.; Stoian, S. A.; Richman, J. E.; Münck, E.; Lipscomb, J. D.; Wackett, L. P. Cyanobacterial Aldehyde Deformylase Oxygenation of Aldehydes Yields n − 1 Aldehydes and Alcohols in Addition to Alkanes. *ACS Catal.* **2013**, *3*, 2228−2238.
(33) Zhang, X.; Rodgers, M. A. J. Energy and Electron Transfer Reactions of the MLCT State of Ruthenium Tris(bipyridyl) with Molecular Oxygen: A Laser Flash Photolysis Study. *J. Phys. Chem.* **1995**, *99*, 12797−12803.
(34) Das, D.; Ellington, B.; Paul, B.; Marsh, E. N. G. Mechanistic Insights from Reaction of α-Oxiranyl-Aldehydes with Cyanobacterial Aldehyde Deformylating Oxygenase. *ACS Chem. Biol.* **2014**, *9*, 570−577.
(35) Park, A. K.; Kim, I.-S.; Jeon, B. W.; Roh, S. J.; Ryu, M.-Y.; Baek, H.-R.; Jo, S.-W.; Kim, Y.-S.; Park, H.; Lee, J. H.; Yoon, H.-S.; Kim, H.-W. Crystal structures of aldehyde deformylating oxygenase from Limnothrix sp. KNUA012 and Oscillatoria sp. KNUA011. *Biochem. Biophys. Res. Commun.* **2016**, *477*, 395−400.
(36) Gray, H. B.; Winkler, J. R. Hole hopping through tyrosine/tryptophan chains protects proteins from oxidative damage. *Proc. Natl. Acad. Sci. U. S. A.* **2015**, *112*, 10920−10925.
(37) Minnihan, E. C.; Nocera, D. G.; Stubbe, J. Reversible, Long-Range Radical Transfer in E. coli Class Ia Ribonucleotide Reductase. *Acc. Chem. Res.* **2013**, *46*, 2524−2535.
(38) Ravichandran, K. R.; Taguchi, A. T.; Wei, Y.; Tommos, C.; Nocera, D. G.; Stubbe, J. A > 200 meV Uphill Thermodynamic Landscape for Radical Transport in Escherichia coli Ribonucleotide Reductase Determined Using Fluorotyrosine-Substituted Enzymes. *J. Am. Chem. Soc.* **2016**, *138*, 13706−13716.
(39) Ravichandran, K. R.; Zong, A. B.; Taguchi, A. T.; Nocera, D. G.; Stubbe, J.; Tommos, C. Formal Reduction Potentials of Difluorotyrosine and Trifluorotyrosine Protein Residues: Defining the Thermodynamics of Multistep Radical Transfer. *J. Am. Chem. Soc.* **2017**, *139*, 2994−3004.
(40) Gray, H. B.; Winkler, J. R. Electron tunneling through proteins. *Q. Rev. Biophys.* **1999**, *36*, 341−372.
(41) Warren, J. J.; Tronic, T. A.; Mayer, J. M. Thermochemistry of Proton-Coupled Electron Transfer Reagents and its Implications. *Chem. Rev.* **2010**, *110*, 6961−7001.
(42) Xue, G.; Wang, D.; De Hont, R.; Fiedler, A. T.; Shan, X.; Münck, E.; Que, L. A synthetic precedent for the $[Fe^{IV}_2(\mu\text{-}O)_2]$ diamond core proposed for methane monooxygenase intermediate Q. *Proc. Natl. Acad. Sci. U. S. A.* **2007**, *104*, 20713−20718.

DOI: 10.1021/acs.inorgchem.8b00673
Inorg. Chem. XXXX, XXX, XXX−XXX

(43) Note that this is a different driving force than for direct reduction of the site by an external electron donor (e.g., ferredoxin). Additional analysis is presented in the Supporting Information.
(44) Bottin, H.; Lagoutte, B. Ferrodoxin and flavodoxin from the cyanobacterium Synechocystis sp PCC 6803. *Biochim. Biophys. Acta, Bioenerg.* **1992**, *1101*, 48−56.
(45) Gregg, E. C.; Tyler, W. P. Polarography of the Bis-(diethylthiocarbamyl) Disulfide—Diethyldithiocarbamate Ion Oxidation—Reduction System. *J. Am. Chem. Soc.* **1950**, *72*, 4561−4565.
(46) Wang, D. L.; Holz, R. C.; David, S. S.; Que, L.; Stankovich, M. T. Electrochemical properties of the diiron core of uteroferrin and its anion complexes. *Biochemistry* **1991**, *30*, 8187−8194.
(47) Silva, K. E.; Elgren, T. E.; Que, L.; Stankovich, M. T. Electron Transfer Properties of the R2 Protein of Ribonucleotide Reductase from Escherichia coli. *Biochemistry* **1995**, *34*, 14093−14103.
(48) With equation 2 and a distance of 18−25 Å for the ADO/petF precursor complex, these E° estimates are consistent with the known ET rate of reduction of ADO by petF.[10]

DOI: 10.1021/acs.inorgchem.8b00673
Inorg. Chem. XXXX, XXX, XXX−XXX